Reviews

Lewis Acidic Behavior of Fluorinated Organomercurials

Thomas J. Taylor, Charlotte N. Burress, and François P. Gabbaï*

Department of Chemistry, Texas A&M University, 3255 TAMU, College Station, Texas 77843-3255

Received February 8, 2007

Owing to their unusual Lewis acidic properties, the coordination chemistry of fluorinated organomercurials is attracting increasing interest. In this review, the authors focus on the synthesis, structures, and properties of neutral Lewis adducts involving fluorinated organomercurials such as $(CF_3)_2Hg$, $(C_6F_5)HgCl$, $(C_6F_5)_2Hg$, and $[(o\text{-}C_6F_4)Hg]_3$. While most of these organomercurials form adducts with common Lewis basic organic substrates, $[(o\text{-}C_6F_4)Hg]_3$ also interacts with aromatic hydrocarbons, alkynes, N-heterocycles, and metallocenes to form π-complexes. In some cases, this complexation mode results in the formation of supramolecules with unusual luminescence properties or microporosity.

Introduction

Organomercurials, which have been known for over 150 years,[1−5] are common reagents in both organic and organometallic chemistry.[6] Despite their linear geometry and apparent unsaturation, the mercury atoms of such compounds exhibit little coordination ability.[7] Although several adducts involving organomercurials have been isolated, both structural and spectroscopic studies have served to confirm the absence of significant Lewis acidity. For example, in its adduct with 2,9-dimethyl-1,10-phenantroline, the mercury atom of diphenylmercury retains a linear C−Hg−C geometry, indicating extremely weak Hg···N interactions.[8] Comparable results have been obtained in the chemistry of organomercury halide derivatives such as MeHgCl, which only forms very labile anionic complexes in the presence of halide anions in solution.[9] This chemical trait may be traced back to the diffuseness and energy of the vacant mercury orbitals, which preclude favorable interactions with the filled orbitals of the donor. Moreover, because mercury and carbon have comparable Pauling electronegativity ($\chi_{(Hg)} = 2.00$, $\chi_{(C)} = 2.55$), the mercury atoms of organomercurials do not accumulate a significant positive character and therefore fail to engage in strong electrostatic interactions with electron-rich substrates.

This situation can be altered upon fluorination of the organic substituents. Early evidence for the Lewis acidic behavior of fluorinated organomercurials was obtained by Emeléus and Lagowski, who found that addition of alkali iodide to $(CF_3)_2Hg$ or CF_3HgI results in the precipitation of salts that contain the $[(CF_3)_2HgI_2]^{2-}$ and $[(CF_3)HgI_2]^-$ anions.[10,11] Further evidence for the Lewis acidic behavior of such compounds came from conductometric titrations, which, for example, showed the formation of 1:1 and 2:1 halide complexes involving $(CF_3)_2Hg$.[10,11] In addition, Seyferth and co-workers demonstrated that the reaction of iodide ions with fluorinated organomercurials such as CF_3HgI and $PhHgCF_3$ leads to extrusion of difluorocarbene,[12] suggesting the nucleophilic displacement of the $[CF_3]^-$ anion by the iodide ion.[13] These seminal contributions were followed by numerous reports that firmly established the affinity of fluorinated organomercurials not only for anionic[7,14−18] but also for neutral electron-rich substrates. Indeed oscillometric titrations indicate that mercurials such as $(CF_3)_2Hg$, $(CF_3CF_2)_2Hg$, $((CF_3)_2CF)_2Hg$, $(CF_3CH_2)_2Hg$, and $(CF_3CHF)_2Hg$ form both 1:1 and 2:1 complexes with neutral bases such as piperidine, dimethyl sulfoxide (DMSO), and pyridine *N*-oxide in benzene solutions.[19] Despite their documented lability, some of these complexes including $[(CF_3)_2Hg(ONC_5H_5)_2]$ and $[(CF_3CHF)_2Hg(OSC_4H_8)_2]$ could be obtained as pure species and characterized by IR and elemental analysis.[20]

These early investigations confirmed that fluorinated organomercurials are indeed Lewis acids. Unlike many Lewis acids, however, fluorinated organomercurials are air- and water-stable, which greatly facilitates their handling and use. Another important distinction comes from the polarizability of the

(1) Seyferth, D. *Organometallics* **2001**, *20*, 2940.
(2) Frankland, E. *Philos. Trans.* **1852**, *142*, 417.
(3) Frankland, E. *Philos. Trans.* **1853**, *85*, 329.
(4) Frankland, E. *J. Chem. Soc.* **1863**, *16*, 415.
(5) Frankland, E. *Ann.* **1864**, *130*, 104.
(6) Gabbaï, F. P.; Melaimi, M.; Burress, C. N.; Taylor, T. J. *Mercury and Cadmium*; Elsevier: Oxford, 2006.
(7) Korpar-Colig, B.; Popovic, Z.; Bruvo, M.; Vickovic, I. *Inorg. Chim. Acta* **1988**, *150*, 113.
(8) Canty, A. J.; Gatehouse, B. M. *Acta Crystallogr., Sect. B* **1972**, *28*, 1872.
(9) Goggin, P. L.; Goodfellow, R. J.; Hurst, N. W. *Dalton Trans.* **1978**, 561.
(10) Emeleus, H. J.; Lagowski, J. J. *Proc. Chem. Soc.* **1958**, 231.
(11) Emeleus, H. J.; Lagowski, J. J. *J. Chem. Soc.* **1959**, 1497.
(12) Seyferth, D.; Hopper, S. P. *J. Org. Chem.* **1972**, *37*, 4070.
(13) Seyferth, D.; Gordon, M. E.; Mui, J. Y. P.; Burlitch, J. M. *J. Am. Chem. Soc.* **1967**, *89*, 959.
(14) Shur, V. B.; Tikhonova, I. A. *Russ. Chem. Bull.* **2003**, *52*, 2539.
(15) Shur, V. B.; Tikhonova, I. A.; Dolgushin, F. M.; Yanovsky, A. I.; Struchkov, Y. T.; Volkonsky, A. Y.; Solodova, E. V.; Panov, S. Y.; Petrovskii, P. V.; et al. *J. Organomet. Chem.* **1993**, *443*, C19.
(16) Naumann, D.; Schulz, F.; Pantenburg, I.; Tyrra, W. *Z. Anorg. Allg. Chem.* **2004**, *630*, 529.
(17) Viets, D.; Lork, E.; Watson, P. G.; Mews, R. *Angew. Chem., Int. Ed. Engl.* **1997**, *36*, 623.
(18) Schulz, F.; Pantenburg, I.; Naumann, D. *Z. Anorg. Allg. Chem.* **2003**, *629*, 2312.
(19) Powell, H. B.; Maung, M. T.; Lagowski, J. J. *J. Chem. Soc.* **1963**, 2484.
(20) Powell, H. B.; Lagowski, J. J. *J. Chem. Soc., Sect. A* **1966**, 1282.

10.1021/om070125d CCC: $37.00
Publication on Web 09/29/2007

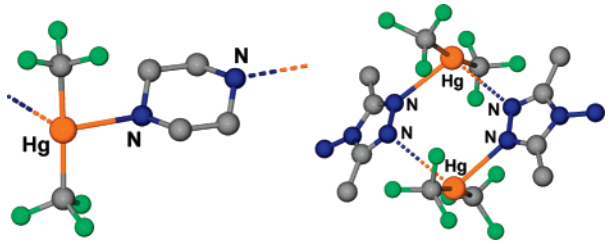

Figure 1. Structure [1·piperazine] and [1·3,5-dimethyl-4′-aminotriazole].

Chart 1. Monofunctional Organomercurials Discussed in This Section

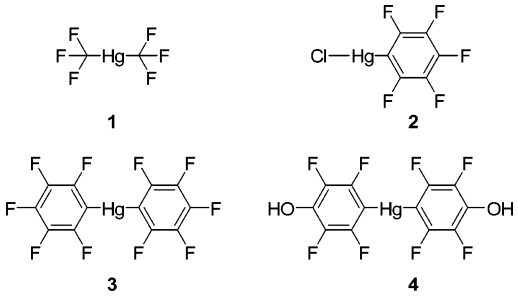

Chart 2. [1·terpy] (left) and [1·crown-6] (right) Adduct of 1

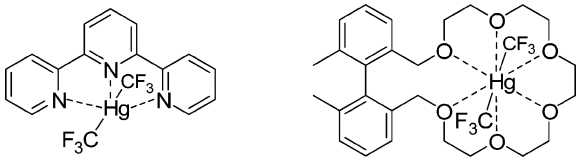

mercury atom, which greatly "softens" the Lewis acidic properties of these derivatives. The purpose of this article is to review the unusual Lewis acidic properties that fluorinated organomercurials display toward neutral substrates.

Lewis Acidic Properties of Monofunctional Organomercurials

As stated in the Introduction, evidence for the formation of adducts involving fluorinated organomercurials and neutral Lewis bases was obtained more than half a century ago. While the composition of these adducts was confirmed beyond any doubts, a clear understanding of the coordination geometry of the mercury center could not be provided. The availability of X-ray diffraction methods has helped to answer some of these questions. Complexes of $(CF_3)_2Hg$ (**1**, Chart 1) that have been recently structurally characterized include the polymeric adduct [**1**·piperazine][21] and the dimeric adduct [**1**·3,5-dimethyl-4′-aminotriazole] (Figure 1).[22] Both of these adducts possess four-coordinate mercury centers in heavily distorted tetrahedral coordination geometries. In both structures, the C−Hg−C angle (171° for [**1**·piperazine] and 173° for [**1**·3,5-dimethyl-4′-aminotriazole]) shows only a modest deviation from linearity, with Hg···N bond distances (2.682 Å for [**1**·piperazine] and 2.72−2.74 Å for [**1**·3,5-dimethyl-4′-aminotriazole]) that are commensurate with the presence of secondary interactions. A stronger complexation of the mercury center is observed in the 2,2′:6′,2″-terpyridyl adduct of $(CF_3)_2Hg$ ([**1**·terpy], Chart 2), which displays increased bending of the C−Hg−C angle

(21) Nolte, M.; Pantenburg, I.; Meyer, G. *Z. Anorg. Allg. Chem.* **2005**, *631*, 2923.
(22) Nockemann, P.; Schulz, F.; Naumann, D.; Meyer, G. *Z. Anorg. Allg. Chem.* **2005**, *631*, 649.

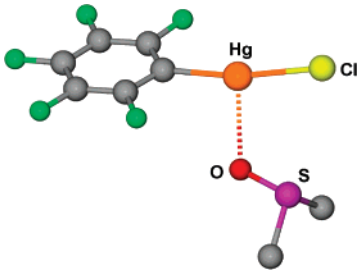

Figure 2. Structure of [**2**·DMSO].

Chart 3

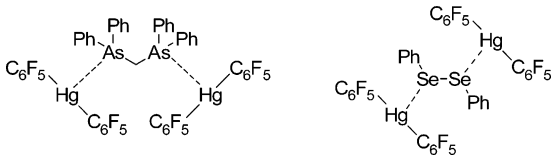

(164.2°) and shorter Hg···N distances (2.62−2.70 Å).[23] Another structure that deserves comment is that of a dimethylbiphenyl crown-6 ether adduct of **1** (denoted as [**1**·crown-6], Chart 2), in which the mercury center interacts with the oxygen atoms of the ligands via weak Hg···O secondary interactions ranging from 2.84 to 3.12 Å.[24,25] Because of the symmetry of these interactions, the C−Hg−C angle (177.9°) remains essentially linear.

The formation of adducts also occurs with fluorinated arylmercury compounds such as pentafluorophenylmercury chloride (**2**, Chart 1), which complexes both dimethylformamide (DMF) and DMSO.[26] The DMSO adduct [**2**·DMSO] has a T-shaped structure, with a relatively short Hg···O bond of 2.542(4) Å (Figure 2). Formation of this short bond is accompanied by a distinct deviation of the C−Hg−Cl angle (169.7(2)°) from linearity. The adduct $[(\mathbf{2})_2\cdot DMF]$ has also been structurally characterized. In this case, however, the DMF molecules bridge two mercury centers via elongated Hg···O interactions in the 2.66−2.85 Å range. In both adducts, intermolecular Hg···Cl secondary interactions connect the individual molecules into extended polymeric structures. These secondary Hg···Cl interactions partly neutralize the Lewis acidity of the mercury centers and can be regarded as competing with the DMSO or DMF ligands. Nonetheless, the coordination of the oxygen to the mercury center results in a noticeable weakening of the sulfoxide (1019 cm^{-1} in [**2**·DMSO] vs 1057 cm^{-1} in free DMSO) and carbonyl (1654 cm^{-1} in $[(\mathbf{2})_2\cdot DMF]$ vs 1675 cm^{-1} in free DMF) IR stretching bands. A few Lewis adducts of bis(pentafluorophenyl)mercury (**3**, Chart 1) have also been reported. These include a 2:1 adduct that involves the bis(diphenylarsino)methane ligand (Chart 3). In this adduct, the arsenic atoms of the ligand are each coordinated to a molecule of **3** via As−Hg interactions of 3.40 Å.[27] This distance can be compared to the Hg···Se distance of 3.48 Å found in the adduct involving **3** and 2,2′-dipyridyl diselenide (Chart 3).[28] The formation of a water adduct of $Hg(C_6F_4OH\text{-}p)_2$ (**4**, Chart 1) has also been

(23) Kamenar, B.; Korpar-Colig, B.; Hergold-Brundic, A.; Popovic, Z. *Acta Crystallogr., Sect. B* **1982**, *38*, 1593.
(24) Rebek, J., Jr.; Costello, T.; Marshall, L.; Wattley, R.; Gadwood, R. C.; Onan, K. *J. Am. Chem. Soc.* **1985**, *107*, 7481.
(25) Onan, K.; Rebek, J., Jr.; Costello, T.; Marshall, L. *J. Am. Chem. Soc.* **1983**, *105*, 6759.
(26) Tschinkl, M.; Schier, A.; Riede, J.; Gabbaï, F. P. *Organometallics* **1999**, *18*, 2040.
(27) Canty, A. J.; Gatehouse, B. M. *Dalton Trans.* **1972**, 511.
(28) Kienitz, C. O.; Thone, C.; Jones, P. G. *Inorg. Chem.* **1996**, *35*, 3990.

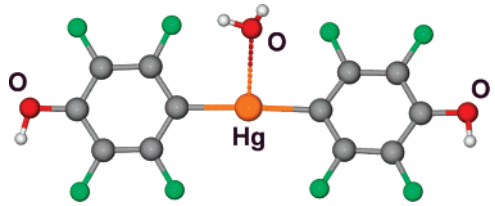

Figure 3. Structure of [**4**·H_2O].

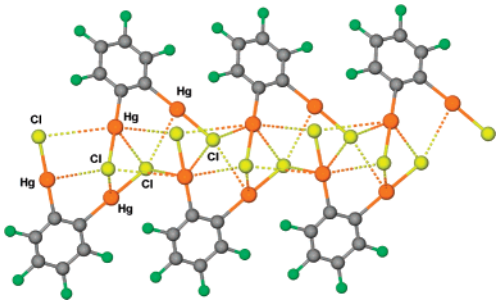

Figure 4. Structure of the base-free form of the pure of **5**.

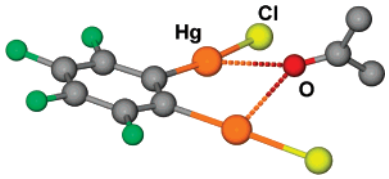

Figure 5. Structure of [**5**·μ_2-acetone].

recently reported (Figure 3).[29] In this adduct, the water ligand forms an Hg···O distance of 3.13 Å, which by far exceeds the Hg···O distances observed in [**2**·DMSO] and [(**2**)$_2$·DMF]. This long distance indicates that the water molecule, which happens to be hydrogen-bonded to the hydroxyl group of a neighboring (C_6F_4OH-*p*) ligand, interacts only weakly with the mercury center.

Lewis Acidic Properties of 1,2-Bis(chloromercurio)-tetrafluorobenzene and Related Compounds

Polydentate Lewis acids have attracted a great deal of attention for the multiple electrophilic activation of organic substrates in various reactions.[30−35] Although such an activation mode has often been proposed, indubitable proof of the concomitant coordination of an organic substrate to two or more Lewis acids remained extremely scarce until Wuest showed that compounds containing the 1,2-bis(mercury)benzene motifs crystallize from formamide solvents to yield complexes in which the carbonyl oxygen atom is coordinated to two and sometimes four mercury centers.[36−43] Since nonfluorinated monofunctional

Chart 4. Bifunctional Organomercurials Discussed in This Section

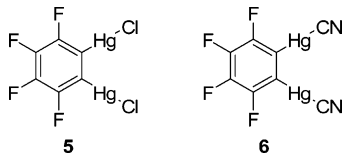

Chart 5. 1:1 and 2:1 Chelate Complexes Formed by 5

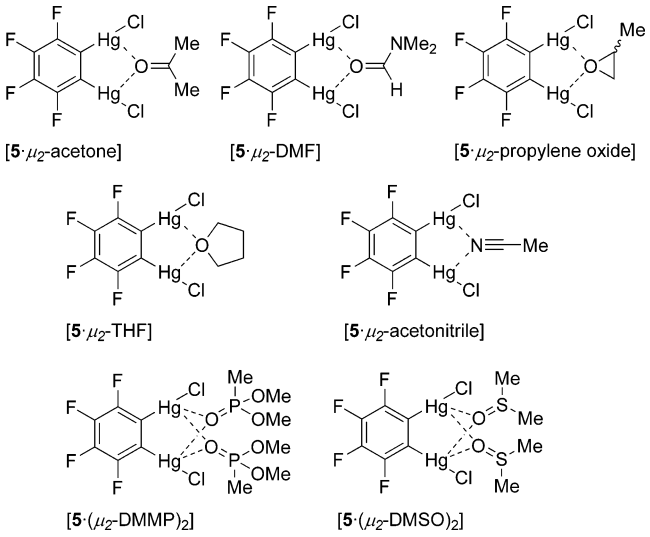

organomercurials do not form isolable adducts with Lewis bases such as formamides, these original results clearly established that the Lewis acidity of polydentate organomercurials is increased by cooperative effects. Analogous results in the chemistry of 1,8-bis(chloromercurio)naphthalene confirmed these findings.[44] Unfortunately, these nonfluorinated bidentate Lewis acids did not form stable adducts with more synthetically useful substrates such as aldehydes and ketones. These limitations led several groups to consider multidentate mercury Lewis acids whose acceptor properties are increased by fluorination of the organic backbone.[14,45]

1,2-Bis(chloromercurio)tetrafluorobenzene (**5**, Chart 4) may be the simplest bifunctional fluorinated organomercurial that has been carefully investigated. This compound can be crystallized in a base-free form from acetaldehyde.[46] It possesses two mercury centers separated by about 3.67 Å and forms extended chains connected by secondary intermolecular Hg···Cl interactions (Figure 4). Titration experiments monitored by ^{199}Hg NMR spectroscopy indicate that this derivative forms weak 1:1 complexes with DMF and DMSO in acetone.[47] The weakness of these complexes may be due to the acetone solvent, which competes for the Lewis acidic mercury sites. In fact, the complex [**5**·μ_2-acetone] can be obtained by slow evaporation of an acetone solution of **5** (Chart 5, Figure 5).[47] Similar crystallization techniques can be used to obtain [**5**·μ_2-DMF] (Chart 5). Structural characterization of these complexes confirms that the

(29) Deacon, G. B.; Felder, P. W.; Junk, P. C.; Muller-Buschbaum, K.; Ness, T. J.; Quitmann, C. C. *Inorg. Chim. Acta* **2005**, *358*, 4389.
(30) Maruoka, K. *Catal. Today* **2001**, *66*, 33.
(31) Ooi, T.; Takahashi, M.; Yamada, M.; Tayama, E.; Omoto, K.; Maruoka, K. *J. Am. Chem. Soc.* **2004**, *126*, 1150.
(32) Oh, T.; Lopez, P.; Reilly, M. *Eur. J. Org. Chem.* **2000**, 2901.
(33) Lopez, P.; Oh, T. *Tetrahedron Lett.* **2000**, *41*, 2313.
(34) Lee, H.; Diaz, M.; Hawthorne, M. F. *Tetrahedron Lett.* **1999**, *40*, 7651.
(35) Reilly, M.; Oh, T. *Tetrahedron Lett.* **1994**, *35*, 7209.
(36) Wuest, J. D. *Acc. Chem. Res.* **1999**, *32*, 81.
(37) Vaugeois, J.; Wuest, J. D. *J. Am. Chem. Soc.* **1998**, *120*, 13016.
(38) Vaugeois, J.; Simard, M.; Wuest, J. D. *Organometallics* **1998**, *17*, 1215.
(39) Vaugeois, J.; Simard, M.; Wuest, J. D. *Coord. Chem. Rev.* **1995**, *145*, 55.
(40) Simard, M.; Vaugeois, J.; Wuest, J. D. *J. Am. Chem. Soc.* **1993**, *115*, 370.
(41) Nadeau, F.; Simard, M.; Wuest, J. D. *Organometallics* **1990**, *9*, 1311.
(42) Wuest, J. D.; Zacharie, B. *J. Am. Chem. Soc.* **1987**, *109*, 4714.
(43) Beauchamp, A. L.; Olivier, M. J.; Wuest, J. D.; Zacharie, B. *Organometallics* **1987**, *6*, 153.
(44) Schmidbaur, H.; Oeller, H. J.; Wilkinson, D. L.; Huber, B.; Mueller, G. *Chem. Ber.* **1989**, *122*, 31.
(45) Haneline, M. R.; Taylor, R. E.; Gabbaï, F. P. *Chem.−Eur. J.* **2003**, *9*, 5189.
(46) Beckwith, J. D.; Tschinkl, M.; Picot, A.; Tsunoda, M.; Bachman, R.; Gabbaï, F. P. *Organometallics* **2001**, *20*, 3169.
(47) Tschinkl, M.; Schier, A.; Riede, J.; Gabbaï, F. P. *Organometallics* **1999**, *18*, 1747.

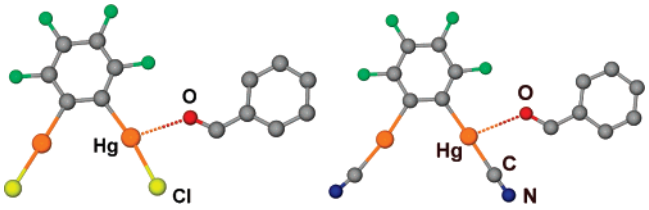

Figure 6. Structure of [**5**·benzaldehyde] (left) and [**6**·benzaldehyde] (right).

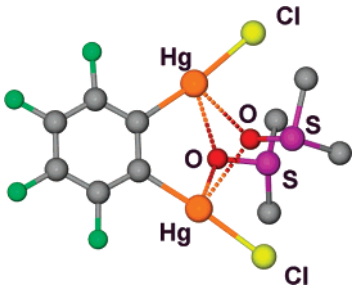

Figure 7. Structure of [**5**·(μ_2-DMSO)$_2$].

oxygen atom is bound to both mercury centers. The resulting Hg···O bonds (2.679(13) and 2.776(14) Å for [**5**·μ_2-acetone]; 2.653(4) Å) and 2.746(4) Å for [**5**·μ_2-DMF]) are shorter than the sum of the van der Waals radii of oxygen and mercury (3.2 Å) and comparable to those observed in [(**2**)$_2$·DMF]. Chelation of the carbonyl oxygen atom results in a weakening of the carbonyl IR stretching frequency by 23 cm^{-1} for [**5**·μ_2-acetone] and 40 cm^{-1} for [**5**·μ_2-DMF]. $^{13}C\{^1H\}$ MAS NMR spectroscopy shows a downfield shift of the carbonyl carbon resonance by 10 ppm for [**5**·μ_2-acetone] and 5 ppm for [**5**·μ_2-DMF] when compared to neat acetone and DMF, respectively.

Crystalline 1:1 complexes of **5** have also been obtained with cyclic ethers such as propylene oxide[46] and THF (Chart 5).[48,49] In both cases, the oxygen is coordinated to both mercury centers. The resulting Hg···O bonds, which fall in the 2.71−2.80 Å range, are slightly longer than those found in the acetone and DMF adducts. Another weak complex is formed with acetonitrile ([5·μ_2-acetonitrile], Chart 5).[46] This complex, which features long Hg···N distances of 2.82(1) and 2.93(1) Å and an essentially unaffected ν_{CN} of 2255 cm^{-1}, is labile and rapidly loses acetonitrile when exposed to air. Interestingly, all aldehyde adducts characterized thus far do not adopt chelate structures. While acetaldehyde does not form any adducts with **5**, the complex [**5**·benzaldehyde] shows only terminal ligation of the carbonyl functionality to one of the mercury atoms via an Hg···O bond of 2.68 Å (Figure 6).[46] Complexes of 2:1 stoichiometry have also been observed with **5** and dimethylmethylphosphonate (DMMP)[50] and DMSO[51] as substrates (Chart 5, Figure 7). In these complexes, the donor ligands are positioned on either side of the approximately planar bidentate Lewis acid. The presence of two donors does not influence the Hg···O bond lengths (av 2.79 Å for [**5**·(μ_2-DMMP)$_2$]); av 2.70 Å for [**5**·(μ_2-DMSO)$_2$]), which are comparable to those observed in 1:1 adducts such as [**5**·μ_2-acetone]. As observed for [**2**·DMSO] and [(**2**)$_2$·DMF], the individual molecules of all adducts shown in Chart 5 contain secondary Hg···Cl interactions and form extended structures. In the case of [**5**·(μ_2-DMSO)$_2$], these

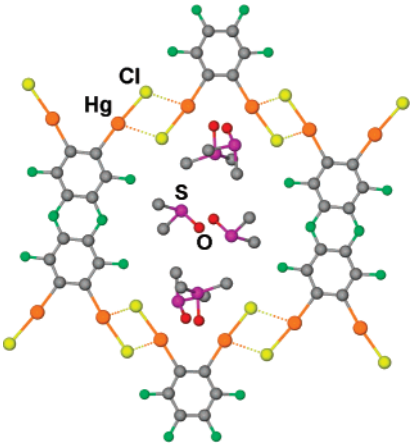

Figure 8. View of a micropore formed in the structure of [**5**·(μ_2-DMSO)$_2$]-DMSO.

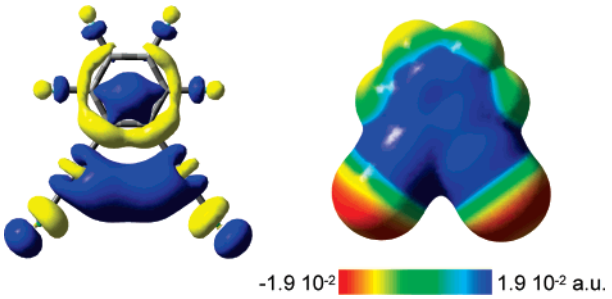

Figure 9. LUMO (isodensity 0.03) and electrostatic potential surface of **5**.

intermolecular Hg···Cl interactions lead to the formation of a microporous molecular lattice whose channels are filled with solvate DMSO molecules (Figure 8).[51]

1,2-Bis(cyanomercurio)tetrafluorobenzene (**6**, Chart 4) reacts with aldehydes to afford complexes such as [**6**·acetaldehyde] and [**6**·benzaldehyde], in which the aldehyde is terminally ligated to one of the mercury centers.[52] The Hg···O bond in [**6**·benzaldehyde] (3.009(12) Å, Figure 6) is noticeably longer than that found in [**5**·benzaldehyde] (2.68 Å). This difference suggests that the cyanide ligand is less electronegative than chloride. The ability of compound **6** to catalyze the cyanosilylation of benzaldehyde has also been investigated. The results of these studies suggest that bidentate organomercurials such as **6** are not involved in the double electrophilic activation of aldehydes but instead assist in the formation of an activated Lewis acidic silicon species by anion complexation.[52]

A geometry optimization of **5** using DFT methods (bp86 functional, basis set: 6-31g for C and F atoms, 6-31g(d′) for Cl and Stuttgart RSC 1997 ECP for Hg) affords a structure close to that observed experimentally.[53] These calculations also indicate that the LUMO (Figure 9) bears a large contribution from the C−Hg−Cl σ^* orbital and features a large lobe spanning the two heavy atoms. In addition, the electrostatic potential surface shows an accumulation of positive charge on the mercury atoms. These theoretical investigations suggest that the formation of adducts of **5** results from electron donation from the filled orbitals of the donor into the LUMO of **5**. However, since coordination does not significantly affect the structure of

(48) Tschinkl, M.; Gabbaï, F. P. *J. Chem. Crystallogr.* **2003**, *33*, 595.
(49) Gardinier, J. R.; Gabbaï, F. P. *Dalton* **2000**, 2861.
(50) Tschinkl, M.; Bachman, R. E.; Gabbaï, F. P. *Organometallics* **2000**, *19*, 2633.
(51) Tschinkl, M.; Schier, A.; Riede, J.; Gabbaï, F. P. *Angew. Chem., Int. Ed.* **1999**, *38*, 3547.
(52) King, J. B.; Gabbaï, F. P. *Organometallics* **2003**, *22*, 1275.
(53) Density functional theory (DFT) calculations (full geometry optimization) were carried out with Gaussian03. Frequency calculations carried out on the optimized structure of this compound confirmed the absence of any imaginary frequencies. The frontier orbitals and the electrostatic potential surface were obtained from the optimized geometry.

Chart 6

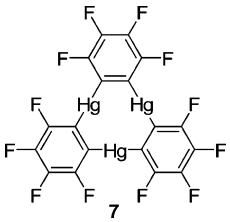

7

Chart 7. Structures and Stoichiometry Adopted by Adducts of 7 with Aldehydes, Ketones, Amides, Nitriles, Phosphoramides, and Sulfoxides

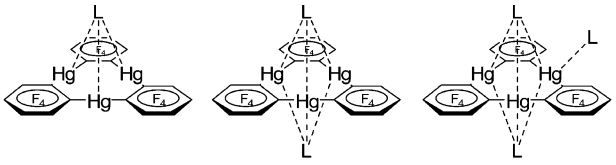

	[**7**·μ_3-L]	[**7**·(μ_3-L)$_2$]	[**7**·(μ_3-L)$_2$(L)]
	*n*PrCN[69]	MeCN[70]	Me_2CO[65]
	CH_2CHCN[70]	PhMeCO[65]	MeCOOEt[67]
L =	MeCHCO[65]	$Me_2N(H)CO$[67,68]	Me_2SO[67]
	Me_2CO[66]	Me_2NMeCO[69]	
	Ph_2CO[65]	$(Me_2N)_3PO$[67]	

the organomercurial and results only in long bonds between the mercury centers and the electron-rich donor atoms, the extent of orbital mixing between the donor and the acceptor must be rather small. In turn, bonding in these adducts most likely bears an important contribution from favorable electrostatic interactions.

Lewis Acidic Properties of Trimeric Perfluoro-*ortho*-phenylene Mercury

Trimeric perfluoro-*ortho*-phenylenemercury (**7**, Chart 6)[54] has been widely investigated as a host for a variety of anions.[14,55−62] This molecule, which can be obtained in a crystalline form by recrystallization from CH_2Cl_2 or sublimation,[63] features a planar structure with readily accessible mercury centers.

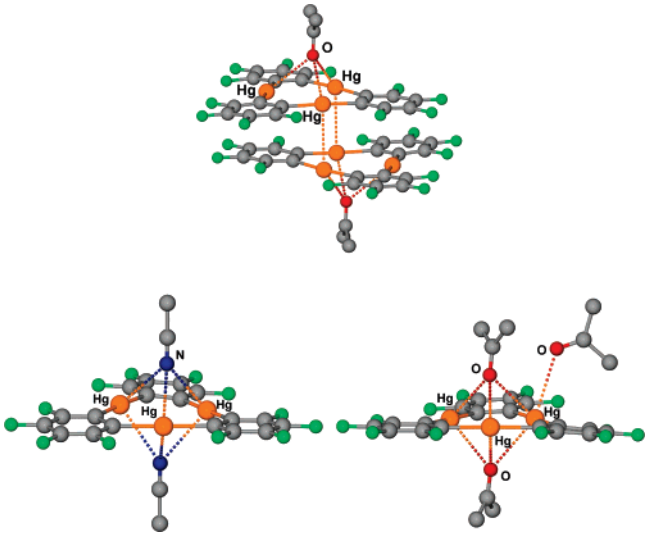

Figure 10. Structure of [**7**·μ_3-acetone] (top), [**7**·(μ_3-acetonitrile)$_2$] (middle), and [**7**·(μ_3-acetone)$_2$(acetone)] (bottom).

Although this compound was reported to form various adducts by Massey over 20 years ago,[64] it is not until recently that a number of structural studies have shed light on its coordination chemistry. These studies have confirmed that this compound exhibits a rich coordination chemistry toward neutral electron-rich substrates including aldehydes,[65] ketones,[65,66] amides,[67−69] nitriles,[69,70] phosphoramides,[67] and sulfoxides,[67] with which it usually forms discrete [**7**·μ_3-L], [**7**·(μ_3-L)$_2$], and [**7**·(μ_3-L)$_2$(L)] complexes. In the [**7**·(μ_3-L)$_2$] complexes, two molecules of the donor are coordinated to the mercury centers of **7** on either side of the molecular plane (Chart 7). A similar situation is encountered in [**7**·(μ_3-L)$_2$(L)], where an additional ligand is terminally ligated to one of the mercury centers. [**7**·μ_3-acetone][66] and [**7**·(μ_3-acetonitirile)$_2$][70] are representative examples of [**7**·μ_3-L] and [**7**·(μ_3-L)$_2$] adducts, respectively (Figure 10). In the case of [**7**·μ_3-acetone], the molecules form co-facial dimers that are held together by two mercuriophilic interactions of 3.51 Å (Figure 10).

For all carbonyl adducts, the Hg···O distances involving the triply bridging substrates fall within a relatively narrow range of 2.8−3.1 Å and do not show any strong dependence on the stoichiometry of the adducts. For example, the Hg···O distances involving the triply bridging acetone molecules in [**7**·μ_3-acetone] (av 2.90 Å)[66] are close to those in [**7**·(μ_3-acetone)$_2$(acetone)] (av 2.88 Å) (Figure 10).[65] The basicity of the ligand also appears to have little influence on the Hg···O distances. For example, the Hg···O bonds in [**7**·(μ_3-DMF)$_2$] (av 2.87 Å)[67] are close to those observed in [**7**·(μ_3-acetone)$_2$(acetone)]. It remains that these Hg···O bonds are distinctly longer than those measured

(54) Sartori, P.; Golloch, A. *Chem. Ber.-Recl.* **1968**, *101*, 2004.
(55) Tikhonova, I. A.; Dolgushin, F. M.; Tugashov, K. I.; Ellert, O. G.; Novotortsev, V. M.; Furin, G. G.; Antipin, M. Y.; Shur, V. B. *J. Organomet. Chem.* **2004**, *689*, 82.
(56) Shubina, E. S.; Tikhonova, I. A.; Bakhmutova, E. V.; Dolgushin, F. M.; Antipin, M. Y.; Bakhmutov, V. I.; Sivaev, I. B.; Teplitskaya, L. N.; Chizhevsky, I. T.; Pisareva, I. V.; Bregadze, V. I.; Epstein, L. M.; Shur, V. B. *Chem.−Eur. J.* **2001**, *7*, 3783.
(57) Saitkulova, L. N.; Bakhmutova, E. V.; Shubina, E. S.; Tikhonova, I. A.; Furin, G. G.; Bakhmutov, V. I.; Gambaryan, N. P.; Chistyakov, A. L.; Stankevich, I. V.; Shur, V. B.; Epstein, L. M. *J. Organomet. Chem.* **1999**, *585*, 201.
(58) Chistyakov, A. L.; Stankevich, I. V.; Gambaryan, N. P.; Struchkov, Y. T.; Yanovsky, A. I.; Tikhonova, I. A.; Shur, V. B. *J. Organomet. Chem.* **1997**, *536/537*, 413.
(59) Tikhonova, I. A.; Dolgushin, F. M.; Yanovsky, A. I.; Struchkov, Y. T.; Gavrilova, A. N.; Saitkulova, L. N.; Shubina, E. S.; Epstein, L. K.; Furin, G. G.; Shur, V. B. *J. Organomet. Chem.* **1996**, *508*, 271.
(60) Shur, V. B.; Tikhonova, I. A.; Yanovskii, A. I.; Struchkov, Y. T.; Petrovskii, P. V.; Panov, S. Y.; Furin, G. G.; Volpin, M. Y. *Dokl. Akad. Nauk* **1991**, *321*, 1002.
(61) Shur, V. B.; Tikhonova, I. A.; Yanovskii, A. I.; Struchkov, Y. T.; Petrovskii, P. V.; Panov, S. Y.; Furin, G. G.; Vol'pin, M. E. *J. Organomet. Chem.* **1991**, *418*, C29.
(62) Shur, V. B.; Tikhonova, I. A.; Yanovskii, A. I.; Struchkov, Y. T.; Petrovskii, P. V.; Panov, S. Y.; Furin, G. G.; Vol'pin, M. E. *Dokl. Akad. Nauk* **1991**, *321*, 1002.
(63) Haneline, M. R.; Gabbaï, F. P. *Z. Naturforsch., B: Chem. Sci.* **2004**, *59*, 1483.
(64) Ball, M. C.; Brown, D. S.; Massey, A. G.; Wickens, D. A. *J. Organomet. Chem.* **1981**, *206*, 265.
(65) King, J. B.; Tsunoda, M.; Gabbaï, F. P. *Organometallics* **2002**, *21*, 4201.
(66) King, J. B.; Haneline, M. R.; Tsunoda, M.; Gabbaï, F. P. *J. Am. Chem. Soc.* **2002**, *124*, 9350.
(67) Tikhonova, I. A.; Dolgushin, F. M.; Tugashov, K. I.; Petrovskii, P. V.; Furin, G. G.; Shur, V. B. *J. Organomet. Chem.* **2002**, *654*, 123.
(68) Baldamus, J.; Deacon, G. B.; Hey-Hawkins, E.; Junk, P. C.; Martin, C. *Aust. J. Chem.* **2002**, *55*, 195.
(69) Tikhonova, I. A.; Dolgushin, F. M.; Tugashov, K. I.; Furin, G. G.; Petrovskii, P. V.; Shur, V. B. *Russ. Chem. Bull.* **2001**, *50*, 1673.
(70) Tikhonova, I. A.; Dolgushin, F. M.; Yanovsky, A. I.; Starikova, Z. A.; Petrovskii, P. V.; Furin, G. G.; Shur, V. B. *J. Organomet. Chem.* **2000**, *613*, 60.

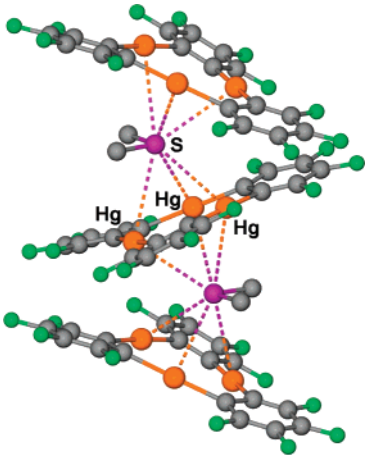

Figure 11. Portion of the coordination polymer observed in [**7**·μ_6-Me_2S]$_n$.

Table 1. IR Data for Selected Adducts of 5 and 7

	$\nu_{C=O}$ of Me_2CO[47,66]	$\nu_{C=O}$ of DMF[47,67,68]	$\nu_{C\equiv N}$ of MeCN[46,70]
5	1693 cm^{-1}	1654 cm^{-1}	2255 cm^{-1}
7	1683 cm^{-1}	1646 cm^{-1}	2266 cm^{-1}
free	1716 cm^{-1}	1675 cm^{-1}	2254 cm^{-1}

in [**5**·μ_2-acetone] (av 2.73 Å) and [**5**·μ_2-DMF] (av 2.70 Å),[47] which is in agreement with the triply rather than doubly bridging location of the carbonyl ligands. Another interesting feature concerns the terminal ligands of [**7**·(μ_3-acetone)$_2$(acetone)], which form relatively long Hg···O bonds of 3.09 Å. This structural feature may be correlated to the lability of the complex, which loses acetone at room temperature.

For all carbonyl adducts reported thus far, coordination to the mercury centers results in a detectable weakening of the carbonyl IR stretching bands. In the acetone and DMF adduct, the weakening effect is more acute than in [**5**·μ_2-acetone] and [**5**·μ_2-DMF],[47] suggesting that the triple coordination of the carbonyl functionality results in an increased polarization of the C═O bond (Table 1). In the case of the nitrile adducts of **7**, coordination leads to an increase in the energy of the nitrile IR stretch. For [**7**·(μ_3-acetonitirile)$_2$], this stretch appears at 2266 cm^{-1}, as opposed to 2255 cm^{-1} in [**5**·μ_2-acetonitrile] and 2254 cm^{-1} in free acetonitrile (Table 1).[46,70] Such an increase has often been observed in Lewis adducts of acetonitrile and is caused by a ligation-induced stabilization of the C≡N σ- and π-bonding orbitals.[71] In turn, the largest deviation observed in [**7**·(μ_3-acetonitirile)$_2$] can be correlated to the triple rather than double coordination of the nitrile functionality.

As expected, this trinuclear complex shows a great affinity for sulfur-containing substrates including dimethyl sulfide. Crystallization of **7** from neat dimethyl sulfide yields [**7**·(μ_3-Me_2S)$_2$(Me_2S)$_2$], in which four molecules of dimethyl sulfide are bound to the trifunctional Lewis acid via Hg···S bonds ranging from 3.2 to 3.5 Å.[72] This complex is quite labile and loses 3 equiv of dimethyl sulfide upon exposure to dry air, thus suggesting the formation of a stable 1:1 adduct. In fact, an adduct of the same stoichiometry can be isolated from 1,2-dichloroethane solutions containing **7** and Me_2S. This adduct, [**7**·μ_6-Me_2S]$_n$, adopts a polymeric structure and contains sandwiched dimethyl sulfide molecules (Figure 11). The sulfur atom of the latter interacts simultaneously with the mercury centers of two neighboring molecules of **7** and thereby achieves hexacoordination. The Hg···S bonds (3.571(3) and 3.543(7) Å) are slightly longer than those observed in [**7**·(Me_2S)$_2$(μ_3-Me_2S)$_2$] for the triply coordinated dimethyl sulfide molecules but remain within the sum of the van der Waals radii. Compound **7** also interacts with bis(2-hydroxyethyl)sulfide to form a 1:1 adduct with a single and relatively short Hg···S bond of 3.14 Å.[73] Several Hg···O interactions also add to the stability of this adduct. Other adducts involving sulfur-containing substrates include [**7**·(μ_3-S═P(OMe)$_2$(*p*-$C_6H_4NO_2$))$_2$][73] and [(**7**)$_2$·TTF] (TTF = tetrathiafulvalene).[74] The latter features a sandwiched TTF molecule held by multiple Hg···S interactions ranging from 3.47 to 3.53 Å.

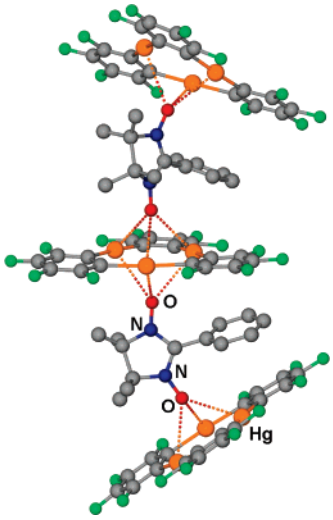

Figure 12. Portion of the coordination polymer observed in [**7**·NIT-Ph]$_n$.

Substrates with at least two accessible Lewis basic sites tend to form more complex aggregates. For example, 2-(phenyl)-4,4,5,5-tetramethylimidazoline-1-oxyl-3-oxide (NIT-Ph) forms either [**7**·NIT-Ph·**7**] or [**7**·NIT-Ph]$_n$ (Figure 12) depending on the stoichiometry of the reaction.[75] In these adducts, each of the oxygen atoms of the NIT-Ph molecule interacts with the mercury centers of an adjacent molecule of **7**. The Hg···O bonds present in these two structures (2.85−3.02 Å) are comparable to those discussed for the carbonyl adducts. Despite the presence of these relatively short bonds, the NIT-Ph molecules of the polymer [**7**·NIT-Ph]$_n$ do not appear to be coupled to one another, as indicated by magnetic susceptibility measurements. This observation suggests that the bonding in such adducts is dominated by electrostatic rather than covalent interactions.

Sandwich structures are also observed for the *p*-benzoquinone and maleic anhydride adducts.[76] The *p*-benzoquinone adduct features two molecules of **7**, which are each coordinated to one of the carbonyl functionalities (Figure 13). The structure of the maleic anhydride adduct is more complicated. In this adduct, two molecules of maleic anhydride are sandwiched between two molecules of **7**. Each molecule of maleic anhydride is triply coordinated via one of its carbonyl functionalities to one of the molecules of **7** and singly coordinated via its remaining carbonyl functionality to the second mercury complex. The Hg···O bonds present in these two structures (2.92−3.12 Å) are once again comparable to those observed in other adducts of oxygen-containing ligands. Remarkably, trinuclear **7** is able to stabilize

(71) Purcell, K. F.; Drago, R. S. *J. Am. Chem. Soc.* **1966**, *88*, 919.
(72) Tsunoda, M.; Gabbaï, F. P. *J. Am. Chem. Soc.* **2003**, *125*, 10492.
(73) Tsunoda, M.; Gabbaï, F. P. *Heteroat. Chem.* **2005**, *16*, 292.
(74) Haneline, M. R.; Gabbai, F. P. *C. R. Chim.* **2004**, *7*, 871.
(75) Haneline, M. R.; Gabbaï, F. P. *Inorg. Chem.* **2005**, *44*, 6248.
(76) Tikhonova, I. A.; Dolgushin, F. M.; Yakovenko, A. A.; Tugashov, K. I.; Petrovskii, P. V.; Furin, G. G.; Shur, V. B. *Organometallics* **2005**, *24*, 3395.

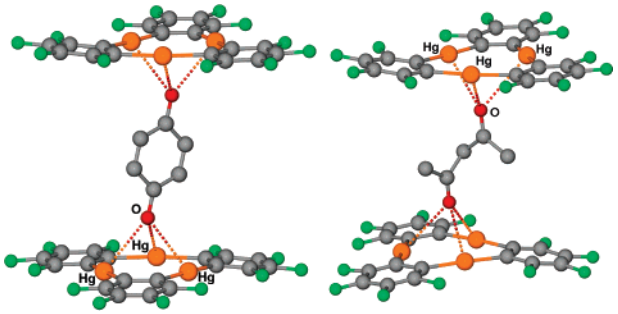

Figure 13. Structure of [(**7**)$_2$·benzoquinone] (left) and [(**7**)$_2$·2,4-pentanedione] (right).

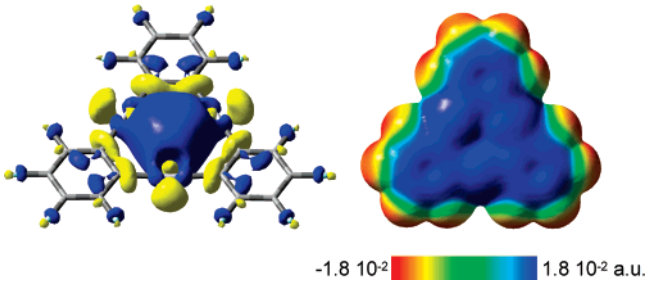

Figure 14. LUMO (0.03 isodensity surface) and electrostatic potential surface of **7**.

Chart 8. Aromatic Hydrocarbons Reported to Form 1:1 Adducts with the Organomercurials 2, 3, and 7

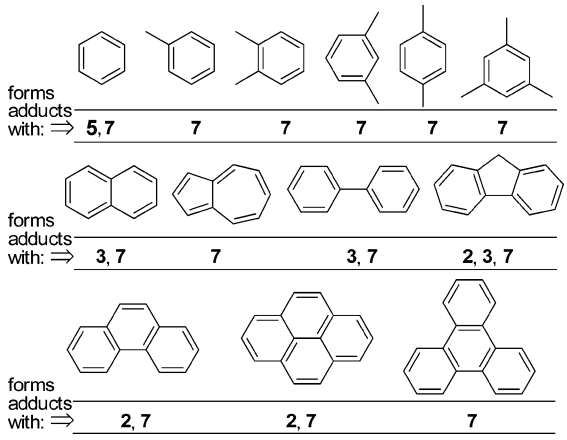

the keto form of acetylacetone (2,4-pentanedione), with which it forms a 2:1 sandwich adduct, which has been structurally characterized (Figure 13). In chloroform solution, dissociation of the adduct occurs and is accompanied by a transformation of the keto form of acetylacetone into a mixture of its tautomers.[77]

Compound **7** has been studied computationally (bp86 functional, basis set: 6-31g for C and F atoms, 6-31g(d′) for Cl, and Stuttgart RSC 1997 ECP for Hg).[53] These calculations indicate that the LUMO spans the three mercury centers and forms a large lobe that protrudes above and below the plane defined by the three mercury atoms (Figure 14). Calculations using all-electron basis sets with the ADF program show that the LUMO bears a large contribution from the mercury 6p orbitals (44%).[75] The presence of this large lobe in the middle of the three mercury centers suggests that this particular region of the molecule is where the Lewis acidity is at a maximum. In agreement with this view, this large lobe appears directly aligned with the direction along which Lewis basic substrates approach the molecule. This simple consideration suggests that formation of adducts possessing triply bridging ligands results from the simultaneous electron donation from the ligand to the three mercury atoms, resulting in four-center−two-electron interactions. However, the computed magnitude of the HOMO−LUMO gap, which is equal to 3.36 eV,[75] indicates that the LUMO might be too high in energy to efficiently mix with the donor orbitals of the ligand. This conclusion is also supported by the cyclic voltammogram of **1** in THF using ^{n}Bu$_4$NPF$_6$ as a supporting electrolyte, which does not show any reduction in the solvent window.[75] As a result, the bonding in these adducts may in fact be dominated by electrostatic rather than covalent interactions. This conclusion is in agreement with the work of Fackler, who showed that the electrostatic potential surface at the center of the trinuclear macrocycle is positive while the periphery is negative (Figure 14).[78] In the case of soft donor atoms such as sulfur, dispersion forces probably add to the stability of the adducts.

Interaction of Fluorinated Organomercurials with Aromatic Hydrocarbons

Arene mercurations are electrophilic substitution reactions which substantiate the strong interactions that can occur between Hg(II) ions and aromatic substrates. Similar conclusions can be derived from the isolation and structural characterization of cationic arene−Hg(II) π-complexes.[79−86] In these complexes, the arene is typically coordinated to the mercury atom in an η^2-fashion via Hg···C$_{arene}$ bonds that range from 2.3 to 2.7 Å. Longer Hg···π interactions are also often observed in neutral organomercurial derivatives that bear arene ligands.[87] With Hg···C$_{arene}$ distances in the range 3 to 3.4 Å, these interactions are inherently weak and have been found to occur mainly in an intramolecular fashion. Examination of the literature shows that simple organomercurials such as Ph$_2$Hg do not form complexes with arenes. As documented in the following paragraphs, this situation can be altered in the presence of fluorinated ligands (Chart 8).

Some of the simplest adducts reported to date involve the organomercurial **2**, which interacts with phenanthrene, fluorene, and pyrene in CHCl$_3$ to form 1:1 adducts, as indicated by elemental analysis (Chart 8).[88] The structure of the phenanthrene adduct has been determined and shows extended binary stacks where molecules of **2** alternate with molecules of phenanthrene (Figure 15). The short Hg···C contacts of 3.29−3.53 Å indicate the presence of secondary Hg−π interactions. These interactions are complemented by perfluoroarene−arene interactions, which

(77) Tikhonova, I. A.; Yakovenko, A. A.; Tugashov, K. I.; Dolgushin, F. M.; Novikov, V. V.; Antipin, M. Y.; Shur, V. B. *Organometallics* **2006**, *25*, 6155.

(78) Burini, A.; Fackler, J. P., Jr.; Galassi, R.; Grant, T. A.; Omary, M. A.; Rawashdeh-Omary, M. A.; Pietroni, B. R.; Staples, R. J. *J. Am. Chem. Soc.* **2000**, *122*, 11264.

(79) Olah, G. A.; Yu, S. H.; Parker, D. G. *J. Org. Chem.* **1976**, *41*, 1983.

(80) Lau, W.; Huffman, J. C.; Kochi, J. K. *J. Am. Chem. Soc.* **1982**, *104*, 5515.

(81) Damude, L. C.; Dean, P. A. W.; Sefcik, M. D.; Schaefer, J. *J. Organomet. Chem.* **1982**, *226*, 105.

(82) Damude, L. C.; Dean, P. A. W. *J. Organomet. Chem.* **1979**, *181*, 1.

(83) Branch, C. S.; Barron, A. R. *J. Am. Chem. Soc.* **2002**, *124*, 14156.

(84) Borovik, A. S.; Barron, A. R. *J. Am. Chem. Soc.* **2002**, *124*, 3743.

(85) Borovik, A. S.; Bott, S. G.; Barron, A. R. *J. Am. Chem. Soc.* **2001**, *123*, 11219.

(86) Borovik, A. S.; Bott, S. G.; Barron, A. R. *Angew. Chem., Int. Ed.* **2000**, *39*, 4117.

(87) Kuzmina, L. G.; Struchkov, Y. T. *Croat. Chem. Acta* **1984**, *57*, 701.

(88) Taylor, T. J.; Burress, C. N.; Pandey, L.; Gabbaï, F. P. *Dalton Trans.* **2006**, 4654.

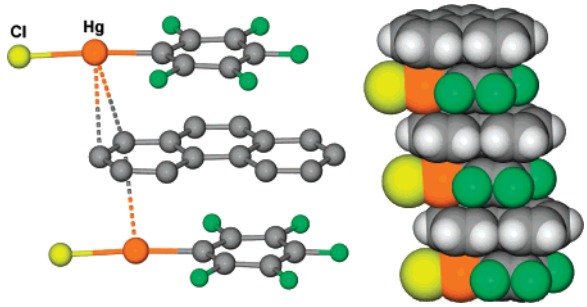

Figure 15. Ball-and-stick (left) and space-filling represenation (right) of a portion of the structure of [2·phenanthrene].

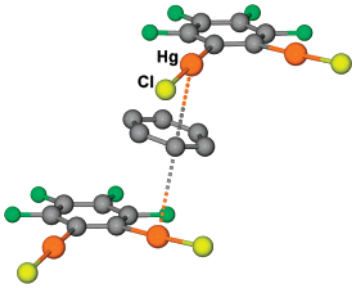

Figure 16. Ball-and-stick representation of a portion of the structure of [**5**·1.5(benzene)].

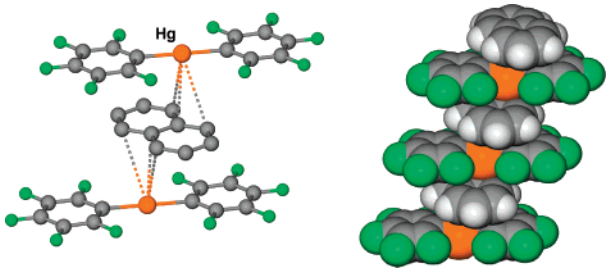

Figure 17. Ball-and-stick (left) and space-filling representation (right) of the structure of [**3**·naphthalene].

presumably add to the stability of the stacks. An even shorter contact is observed in the adduct [**5**·1.5(benzene)], which can be obtained from a propylene oxide solution containing **5** and benzene (Chart 8).[49] The crystal structure of this complex reveals the presence of a η^1-μ-benzene molecule, which bridges the mercury centers of adjacent molecules of **5** (Figure 16). The resulting Hg···C distances of 3.16 and 3.24 Å confirm the presence of an interaction. Examination of the packing diagram also suggests the absence of significant benzene−fluoroarene interactions.

The presence of a mercury chloride moiety does not appear to be a prerequisite for the formation of arene complexes. In fact, a recent study has shown that **3** forms crystalline adducts with a variety of arenes including naphthalene, biphenyl, and fluorene (Chart 8).[89] The solid-state structures of these adducts reveal the existence of supramolecular binary stacks where molecules of **3** alternate with the aromatic substrate. The shortest Hg···C contacts (3.21−3.49 Å) are detected for [**3**·naphthalene], in which the naphthalene interacts with the mercury centers in a bis(trihapto) fashion (Figure 17). Cohesion of the stacks in adducts [**3**·biphenyl] and [**3**·fluorene] can be attributed to both secondary Hg−π and perfluoroarene−arene interactions.

Similar properties are also displayed by the trinuclear complex **7**, which shows a marked affinity for many arenes. For example,

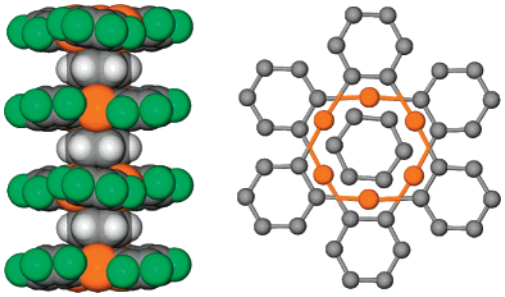

Figure 18. Side and top views of a stack in the structure of [**7**·C_6H_6].

7 crystallizes from benzene to afford extended binary stacks where molecules of **7** alternate with molecules of benzene (Figure 18, Chart 8).[90] These stacks are rather compact (centroid−centroid distance of 3.24 Å) so that secondary π-interactions can be invoked between the benzene molecule and the mercury centers. Each of the six C−C bonds of the benzene molecule interacts with one of the six mercury centers of the two juxtaposed molecules of **7**. The Hg···C contacts must be relatively weak, as no significant differences in the C−C bond lengths of benzene were noted. As indicated by wide-line deuterium NMR spectroscopy, the sandwiched benzene molecules undergo an in-plane 60° reorientation with an activation energy of 52 ± 4 kJ/mol.[45] The magnitude of this activation energy suggests the presence of directional interactions between the mercury atoms of **7** and the benzene molecules.

In order to assess how the bulk of the arene influences the structure of such stacked assemblies, the adducts of **7** with toluene, *o*-, *m*-, and *p*-xylenes, and mesitylene have been synthesized and structurally characterized (Chart 8).[91] In all cases these adducts form extended binary stacks similar to those found in [**7**·benzene]. The substituted benzene molecules adopt an apparently random orientation with respect to the trinuclear core of **7**, thus suggesting that the binding might be largely dispersive and/or electrostatic. Complex **7** also forms adducts with larger aromatic substrates including biphenyl,[92] naphthalene,[92] pyrene,[93] triphenylene,[92] fluorene,[89] azulene,[94] and phenanthrene (Chart 8).[88] As for the benzene and substituted benzene adducts, the structure of the arene derivatives consists of extended stacks where molecules of **7** alternate with the aromatic substrate (Figure 19). In the case of [**7**·triphenylene], arene−fluoroarene contacts between the two components are also present, thus adding to the stability of the stacks. Clues to the formation of some of these adducts in solution can be obtained from fluorescence quenching experiments. For example, addition of **7** to a solution of naphthalene quenches the emission of naphthalene with a Stern-Volmer constant of 159 ± 6 M^{-1}.[89]

In all cases, donor−acceptor interactions between the arene and the Lewis acidic mercury centers may be responsible for the formation of these adducts. Keeping in mind that mercury is polarizable, intense van der Waals interactions cannot be neglected and most certainly contribute to the formation of these supramolecules.

(89) Burress, C. N.; Bodine, M. I.; Elbjeirami, O.; Reibenspies, J. H.; Omary, M. A.; Gabbaï, F. P. *Inorg. Chem.* **2007**, *46*, 1388.
(90) Tsunoda, M.; Gabbaï, F. P. *J. Am. Chem. Soc.* **2000**, *122*, 8335.
(91) Haneline, M. R.; King, J. B.; Gabbaï, F. P. *Dalton Trans.* **2003**, 2686.
(92) Haneline, M. R.; Tsunoda, M.; Gabbaï, F. P. *J. Am. Chem. Soc.* **2002**, *124*, 3737.
(93) Omary, M. A.; Kassab, R. M.; Haneline, M. R.; Elbjeirami, O.; Gabbaï, F. P. *Inorg. Chem.* **2003**, *42*, 2176.
(94) Tikhonova, I. A.; Tugashov, K. I.; Dolgushin, F. M.; Yakovenko, A. A.; Strunin, B. N.; Petrovskii, P. V.; Furin, G. G.; Shur, V. B. *Inorg. Chim. Acta* **2006**, *359*, 2728.

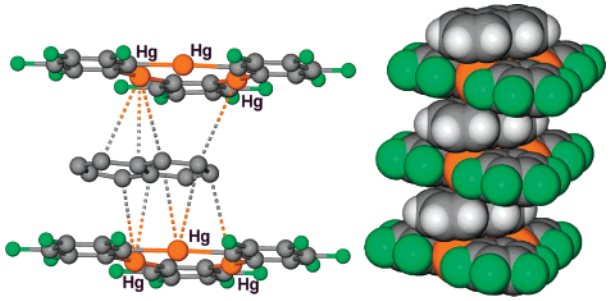

Figure 19. Ball-and-stick (left) and space-filling representation (right) of part of the structure of [7·naphthalene].

Table 2. Radiative Rate Constants and Triplet Lifetimes for Naphthalene, Biphenyl, and Fluorene Adducts of 3 and 7

	k_r/s^{-1}	τ_{4K}/ms	τ_{77K}/ms[a]	τ_{RT}/ms
[**3**·naphthalene]	139	7.71	5.15	3.11
[**3**·biphenyl]	209	4.77	2.96	2.60
[**3**·fluorene]	264	3.32	1.56	0.976
[**7**·naphthalene]	669	1.42	0.985	0.712
[**7**·biphenyl]	1091	0.891	0.337	0.454
[**7**·fluorene]	1469	0.657	0.436	0.265
[**7**·pyrene]			0.423	0.568

[a] For comparison, the triplet lifetimes of pyrene, naphthalene, biphenyl, and fluorene in frozen glasses are 0.7, 2.3, 4.4, and 6.3 *seconds*, respectively.

In the solid state, arene adducts of **2**, **3**, and **7** are photoluminescent and show room-temperature phosphorescence of the arene. The observed phosphorescence results from the spin−orbit coupling provided by the mercury atom, which effectively promotes population of the triplet state of the arene via intersystem crossing. Taking into account the fact that the mercury atoms of the organomercurial are coordinated to the π-faces of the arene, such an external heavy-atom effect seems to constitute a valid explanation for the observed phosphorescence. In all cases, the emission lifetimes are shorter than those of the free arenes (Table 2). Once again, the strong spin−orbit coupling effect caused by the mercury atoms[95] makes the radiative relaxation of the triplet state a more allowed transition, hence leading to shorter lifetimes than those exhibited by the pure organic compounds, in which phosphorescence is strongly forbidden. Arene adducts of these organomercurials constitute promising materials for the development of OLED. Because the emission results only from the triplet state of the arene, emission colors can be tuned simply by varying the identity of the arene substrate. As an example, the pyrene, naphthalene, and biphenyl adducts give rise to a red, blue, and green emission, respectively (Figure 20).

Comparative studies carried out on the naphthalene, biphenyl, and fluorene adducts of **3** and **7** show that the triplet lifetimes measured for adducts involving **7** are distinctly shorter than those recorded for arene adducts of **3**. Accordingly, the triplet radiative decay rate constant of adducts involving **7** are significantly higher than those measured for adducts involving **3** (Table 2). The drastic shortening in the lifetimes and increase in k_r values for arene adducts of **7** versus **3** demonstrate cooperative effects between the three mercury centers in **7** that lead to more efficient phosphorescence via external heavy-atom effects.

Interaction of Fluorinated Organomercurials with N-Heterocycles

The use of triplet emitters in OLED has become an efficient way to improve the electroluminescence efficiency of the device.[96] Unfortunately, triplet lifetimes are typically long and do not always allow for the rapid on/off switching of the emission required in displays. For these reasons, strategies that would afford lifetimes in the microsecond range are receiving considerable attention.[97] Since chromophores with internal spin−orbit perturbation are typically more sensitive to external heavy-atom effects,[98] recent efforts have focused on the synthesis and properties of complexes involving **7** and *N*-methylcarbazole or *N*-methylindole, wherein the nitrogen atom acts as an internal spin−orbit coupling perturber.[99] These recent studies build on an earlier report that clearly established the affinity of **7** for other N-heterocyclic substrates including 4-phenylpyridine.[64]

Binary adducts containing **7** and *N*-methylcarbazole or *N*-methylindole can be readily crystallized from CH_2Cl_2. The structure of [**7**·*N*-methylcarbazole] has been experimentally determined (Figure 21).[100] It resembles the structure of arene adducts of **7** and consists of extended alternating stacks in which the individual components interact via long Hg···N and Hg···C interactions. The emission spectra of the adducts correspond to monomer phosphorescence of the N-heterocycles with lifetimes less than 100 μs at room temperature and 77 K (Figure 21). Remarkably, the lifetimes at 77 K are shortened by 5 orders

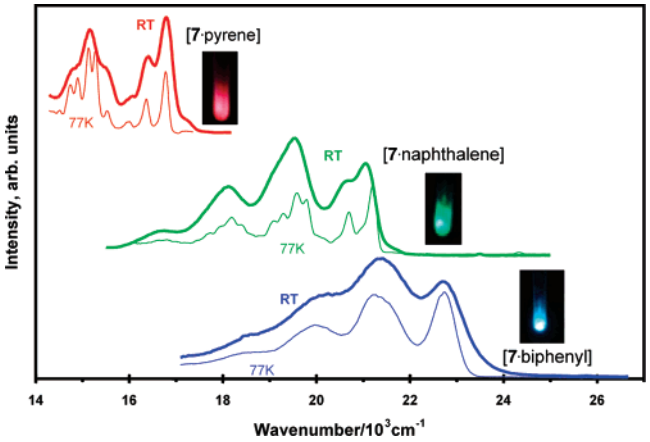

Figure 20. Photoluminescence spectra for crystalline solids of [**7**·pyrene], [**7**·naphthalene], and [**7**·biphenyl]. Intensities of different spectra were adjusted arbitrarily for clarity. Photographs are shown for the emissions of crystalline solids at ambient temperature.

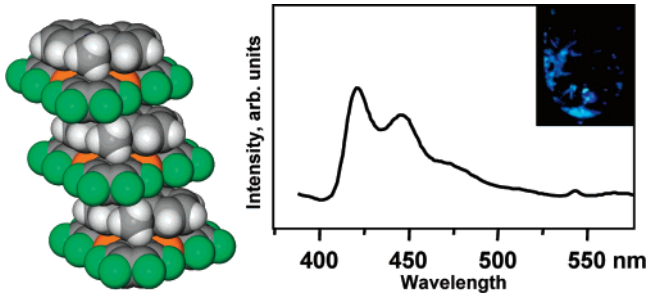

Figure 21. Space-filling view and room-temperature photoluminescence spectrum of [**7**·*N*-methylcarbazole]. The photograph shows the emissions of the solid at ambient temperature under a hand-held UV light.

(95) Griffith, J. S. *Theory of Transition Metal Ions*; Cambridge University Press: Cambridge, 1964.

(96) Baldo, M. A.; Thompson, M. E.; Forrest, S. R. *Pure Appl. Chem.* **1999**, *71*, 2095.

(97) Stoffers, C.; Yang, S.; Zhang, F.; Jacobsen, S. M.; Wagner, B. K.; Summers, C. J. *Appl. Phys. Lett.* **1997**, *71*, 1759.

(98) McGlynn, S. P. *Chem. Rev.* **1958**, *58*, 1113.

(99) Nijegorodov, N.; Mabbs, R. *Spectrochim. Acta, Part A* **2001**, *57*, 1449.

(100) Burress, C.; Elbjeirami, O.; Omary, M. A.; Gabbaï, F. P. *J. Am. Chem. Soc.* **2005**, *127*, 12166.

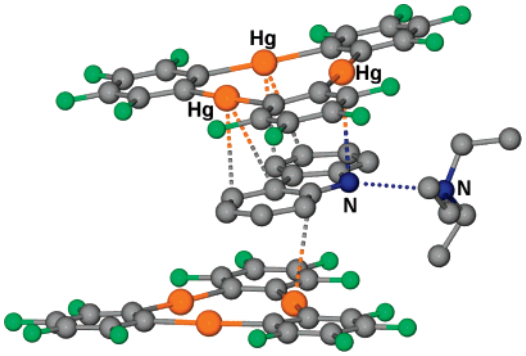

Figure 22. View of part of the structure of [**7**·($C_{12}H_8NH$·NEt_3)].

Table 3. Triplet Lifetimes for N-Heterocycles and Their Adducts with 7

	pure	complexed to **7**	
	EPA	solid, 77 K	solid, RT
N-methylindole	6.7 s	57 μs	29 μs
N-methylcarbazole	7.5 s	99 μs	49 μs

Chart 9. Alkynes Reported to Form Adducts with the Organomercurial 7

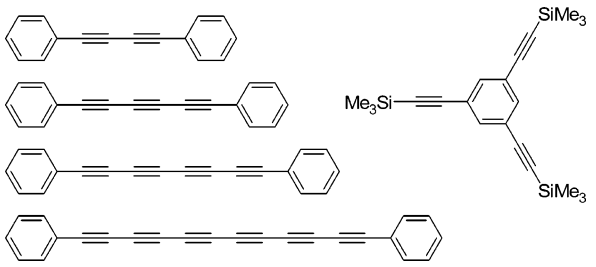

of magnitude when compared to those of the free N-heterocycles in EPA glass (Table 3). Such lifetime reductions are unusual and most likely result from the synergy of the external mercury and internal nitrogen heavy atom effects.

The trinuclear mercury derivative **7** also complexes carbazole to form a binary adduct whose structure has not been elucidated.[101] Interestingly, when **7** and carbazole are combined in the presence of a Lewis base such as THF or NEt_3, the ternary adducts [**7**·($C_{12}H_8NH$·THF)] and [**7**·($C_{12}H_8NH$·NEt_3)] (Figure 22), respectively, can be isolated.[101] In these adducts, the carabazole is hydrogen bonded to the Lewis base. Both adducts have extended structures that exhibit supramolecular binary stacks in which molecules of **1** and the carbazole−Lewis base complex alternate. Since carbazole alone does not form adducts with THF or NEt_3, these results suggest that complexation to **7** increases the acidity of the carbazole substrate.

Interaction of Fluorinated Organomercurials with Alkynes

The interaction of trimeric **7** with α,ω-diphenylpolyynes containing 4, 6, 8, and 12 sp-carbon atoms (Chart 9) in CH_2Cl_2 leads to formation of [(**7**)$_2$·Ph(C≡C)$_2$Ph], [**7**·Ph(C≡C)$_3$Ph], [(**7**)$_2$·Ph(C≡C)$_4$Ph], and [(**7**)$_2$·Ph(C≡C)$_6$Ph·CH_2Cl_2].[102] In the solid state, the α,ω-diphenylpolyynes, which are approximately planar, are associated with molecules of **7** on either side of the molecular plane via secondary Hg···π interactions (Figure 23). The acetylenic stretches of these adducts as measured by IR spectroscopy are essentially identical to those of the free

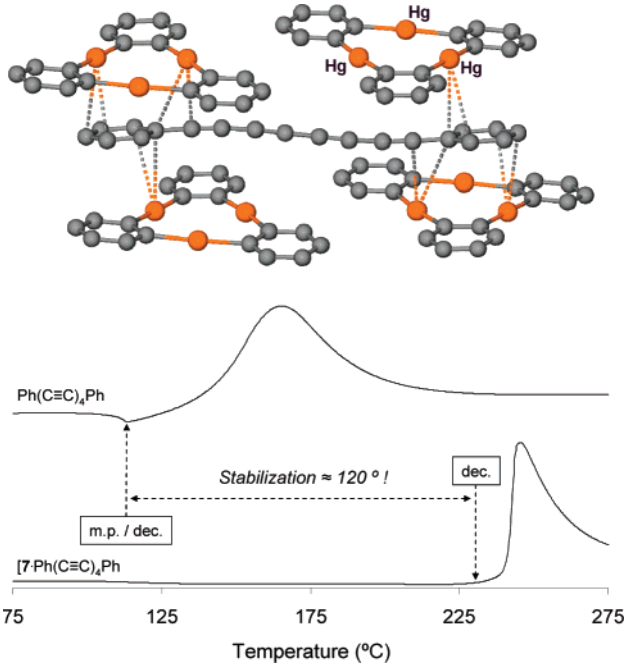

Figure 23. Molecular structure of [**7**·Ph(C≡C)$_4$Ph] and DSC traces of Ph(C≡C)$_4$Ph and [**7**·Ph(C≡C)$_4$Ph] showing the stabilization of the polyyne induced by complexation to **7**.

polyyne. DSC/TGA studies indicate that adducts [(**7**)$_2$·Ph(C≡C)$_2$Ph], [**7**·Ph(C≡C)$_3$Ph], and [(**7**)$_2$·Ph(C≡C)$_4$Ph] are more thermally stable than the respective free α,ω-diphenylpolyynes (Figure 23). For Ph(C≡C)$_4$Ph, the stability range is increased by almost 120 °C in an oxidizing atmosphere. Similar conclusions are derived by monitoring the acetylenic stretch of Ph(C≡C)$_4$Ph and [(**7**)$_2$·Ph(C≡C)$_4$Ph] as a function of temperature in KBr. The increase in stability of the α,ω-diphenylpolyynes in these adducts results from their entrapment and physical separation in a supramolecular lattice. Paradoxically, the supramolecular forces responsible for the formation of these adducts are weak and do not affect the structure of the polyynes.

Compound **7** also reacts with 1,3,5-tris(trimethylsilylethynyl)-benzene (Chart 9) to afford binary columns (Figure 24).[103] These columns are rather compact, as indicated by the distance of 3.28 Å separating the centroids of the two components. Remarkably, these columns display peripheral trimethylsilyl groups and self-aggregate to generate a hexagonal microporous solid featuring 6 Å wide channels. With nonpolar methyl groups decorating their walls, the channels of this solid exhibit a high affinity for alkanes, which are reversibly trapped, as indicated by gravimetric measurements and NMR spectroscopy (Figure 25). Surprisingly, the uptake observed for *n*-butane (2.9 wt %) is greater than that for pentane (2.2 wt %) and hexane (2.2 wt %). Molecular mechanics simulations suggest that this difference results from a more efficient packing of the *n*-butane molecules in the channels. This microporous solid is rather robust, as indicated by gas exchange experiments, which occur with retention of the original structure.

Interaction of Fluorinated Organomercurials with Neutral Inorganic and Organometallic Complexes

Simple mixing of **7** with ferrocene or nickelocene results in the formation of supramolecular electrophilic double-sandwiches

(101) Burress, C. N.; Gabbaï, F. P. *Heteroat. Chem.* **2007**, *18*, 195.
(102) Taylor, T. J.; Gabbaï, F. P. *Organometallics* **2006**, *25*, 2143.
(103) Taylor, T. J.; Bakhmutov, V. I.; Gabbaï, F. P. *Angew. Chem., Int. Ed.* **2006**, *45*, 7030.

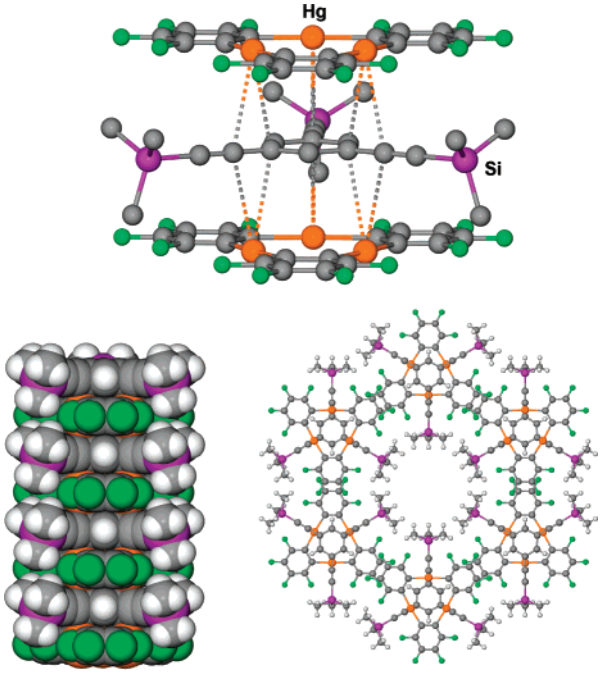

Figure 24. Structure of [**7**·1,3,5-tris(trimethylsilylethynyl)benzene]. Left: ball-and-stick view of a portion of the stacks; middle: space-filling view of a stack showing four repeating units; right: top view of the honeycomb structure of **2** along the *c*-axis showing a micropore.

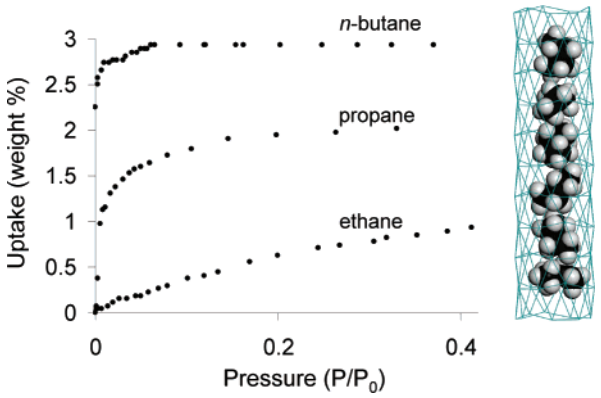

Figure 25. Left: alkane sorption isotherms for [**7**·1,3,5-tris(trimethylsilylethynyl)benzene] at room temperature. Right: arrangements and conformations of the *n*-butane molecules in the channels of [**7**·1,3,5-tris(trimethylsilylethynyl)benzene] derived from MM2 calculations.

in which each cyclopentadienyl ring of the metallocene is capped by a molecule of **7** (Figure 26). The shortest Hg···C distances range from 3.20 to 3.24 Å and indicate that the carbon atoms of the Cp rings are in close contact with the mercury centers.[104] Unlike pure nickelocene, which is air sensitive and displays a green color, the nickelocene adduct [(**7**)$_2$·NiCp$_2$] is air-stable and dark red. The unusual color of this complex results from an increase in the intensity of the formally spin forbidden $^3A_{2g} \rightarrow {}^1E_{1g}$ transition, indicating the occurrence of a mercury heavy-atom effect.

Trinuclear **7** also shows a marked affinity for electron-rich gold complexes including [Au(μ-C$_2$,N$_3$-bzim)]$_3$ (bzim = 1-benzylimidazolate), with which it interacts in solution as indicated by ^{19}F/^{1}H-HOESY and PGSE NMR measurements.[78,105] The

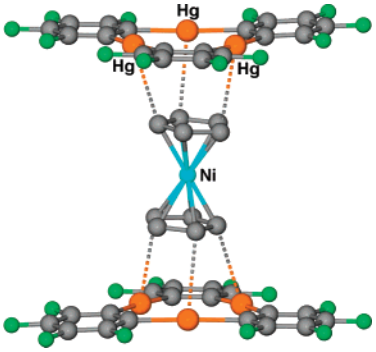

Figure 26. Molecular structure of [(**7**)$_2$·NiCp$_2$].

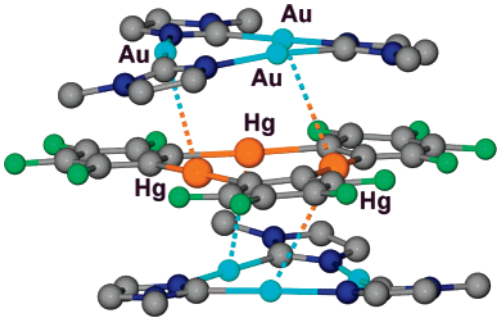

Figure 27. Molecular structure of the 2:1 adduct formed by [Au(μ-C$_2$,N$_3$-bzim)]$_3$ and **7**. The phenyl groups of the benzylimidazolate ligands are omitted.

trinuclear organomercurial **7** crystallizes with two molecules of [Au(μ-C$_2$,N$_3$-bzim)]$_3$ to form extended chains in which the organomercurial is sandwiched between two molecules of the gold complex (Figure 27).[78] Examination of the structure of these complexes shows the presence of metallophilic Hg···Au interactions of 3.27 and 3.24 Å, which appear to be complemented by electrostatic interactions between the π-basic gold complex and the π-acidic mercury derivative.

Conclusion

The results discussed in this review show that the introduction of fluorinated ligands into organomercurials has a dramatic effect on their Lewis acidic properties. This effect most likely results from an increase in the positive charge developed by the mercury atoms along with a lowering of the energy of the vacant orbitals. As a result, fluorinated organomercurials form Lewis adducts with numerous bases. Similar effects can be invoked in the chemistry of mercuracarborands, which also possess Lewis acidic mercury centers.[106,107]

Surprisingly, fluorinated organomercurials also have an affinity for aromatic substrates, alkynes, and N-heterocycles, with which they form unusual π-complexes. In addition to possessing unprecedented structures, these π-complexes show a set of distinctive properties imparted by the presence of the mercury atoms. Specifically, the mercury atoms act as spin−orbit coupling perturbers and trigger the phosphorescence of the π-complexed substrates. This approach is extremely general and is likely to find application in the design of light-emitting devices.

(104) Haneline, M. R.; Gabbaï, F. P. *Angew. Chem., Int. Ed.* **2004**, *43*, 5471.

(105) Burini, A.; Fackler, J. P., Jr.; Galassi, R.; Macchioni, A.; Omary, M. A.; Rawashdeh-Omary, M. A.; Pietroni, B. R.; Sabatini, S.; Zuccaccia, C. *J. Am. Chem. Soc.* **2002**, *124*, 4570.

(106) Wedge, T. J.; Hawthorne, M. F. *Coord. Chem. Rev.* **2003**, *240*, 111.

(107) Hawthorne, M. F.; Zheng, Z. *Acc. Chem. Res.* **1997**, *30*, 267.

Acknowledgment. We would like to thank Dietmar Seyferth for inviting us to write this review as well as the Texas Advanced Technology Program (Grant 010366-0039-2003), the National Science Foundation (Grant CHE-0094264), the American Chemical Society Petroleum Research Fund (Grant 38143-AC 3), and the Welch Foundation (Grant A-1423) for supporting the organomercury research carried out in our laboratory. We also thank our photophysics collaborators Mohammad Omary and Oussama Elbjeirami who generated some of the data presented in this review.

OM070125D